AIAA JOURNAL
Vol. 38, No. 10, October 2000

Effects of Pressure Gradients on Turbulent Boundary Layer Wave Number Frequency Spectra

K. Cipolla* and W. Keith†
U.S. Naval Undersea Warfare Center, Newport, Rhode Island 02841-1708

We extend the work of Schloemer concerning the fluctuating wall pressure field for turbulent boundary layers with mild favorable and adverse pressure gradients (Schloemer, H. H., "Effects of Pressure Gradients on Turbulent-Boundary-Layer Wall-Pressure Fluctuations," *Journal of the Acoustical Society of America*, Vol. 42, No. 1, 1967, pp. 93–113). The use of δ as an outer length scale is shown to produce distinct trends in the convection velocities. The autospectra for the respective cases are scaled on inner and outer variables, with outer variables collapsing the data over a narrow frequency range. The effects of spatial averaging due to the finite transducer size are taken into account. Estimations of the wave number frequency spectra are obtained by spatially transforming the cross spectra, and taking into account the variation of convection velocity with spatial separation. A distinct trend in these spectra are displayed, with an asymmetric convective ridge that broadens as the pressure gradient changes from favorable to adverse. Uncertainties in the estimation of the spectra are discussed. The results are applicable to the flow-induced radiated noise of undersea vehicles and the self-noise of sonar systems.

Nomenclature

d	= wall-pressure sensor diameter
d^+	= nondimensional sensor diameter $= du_\tau/\nu$
$G(\xi, \omega_o)$	= cross spectrum
k	= streamwise wave number
R_θ	= Reynolds number based on momentum thickness $= U_o\theta/\nu$
U_o	= freestream velocity
u_c	= convection velocity
u_τ	= friction velocity $= \sqrt{(\tau_w/\rho)}$
α	= decay constant for the cross spectrum
δ	= boundary-layer thickness
δ^*	= boundary-layer displacement thickness
θ	= boundary-layer momentum thickness
κ	= nondimensional streamwise wave number $= -k\delta$
ν	= kinematic viscosity
ξ	= streamwise separation
$\Phi(\omega_o)$	= autospectrum
$\Phi(k, \omega_o)$	= wave number frequency spectrum
χ	= nondimensional streamwise separation $= \xi/\delta$
ψ	= nondimensional convection velocity $= u_c/U_o$
Ω	= nondimensional frequency $= \omega_o\delta/U_o$
ω	= frequency
$\sim$	= nondimensionalized quantities

I. Introduction

THE turbulent wall pressure field beneath equilibrium flat plate turbulent boundary layers for zero pressure gradient flows has received considerable attention over the past 40 years. Motivation for this research has involved the problem of direct flow noise at the fluid–solid interface as well as flow-induced noise and vibration for aircraft and submarine applications. Designs of sonar systems are aimed at mitigating flow noise and flow-induced noise. The nonintrusive nature of the measurement of wall pressure fluctuations allows experimental investigations into the fundamental physics of turbulence. An inherent complication is the presence of acoustic noise in flow facilities, which, in general, has a negligible effect on the turbulent flow field but contaminates the wall pressure measurements. Traditionally, significant efforts and expense were involved in designing and fabricating acoustically quiet air and water flow facilities. Recent advances in noise cancellation through signal processing have allowed useful measurements in less quiet facilities.

Willmarth[1] provided an early review of the subject, with more recent works by Farabee and Casarella,[2] Keith et al.,[3] and Keith and Abraham[4] focusing on scaling issues and modeling the wave number frequency spectrum. Abraham and Keith[5] recently presented direct measurements of the wave number frequency spectrum, and compared scaling laws using direct measurements of the turbulent boundary layer parameters. Additional attention has focused on the effect of transducer size on the measured wall pressure field. Bull and Thomas,[6] Schewe,[7] and Löfdahl et al.[8] have all addressed this issue through experimental measurements with various sized transducers. The case of wall pressure fluctuations beneath axisymmetric turbulent boundary layers has been addressed by Willmarth and Yang,[9] Lueptow,[10] Snarski and Lueptow,[11] and others. However, the problem of turbulent wall pressure fluctuations beneath flat plate turbulent boundary layers in mild favorable and adverse pressure gradients, considered by Schloemer,[12] has received considerably less attention.

This problem arises in the flow field in the bow and aft region of submarines and surface ships. Schloemer[12] concluded the most striking differences were the changes in the convection velocities resulting from the distortion of the mean velocity profiles imposed by the pressure gradients. In addition, the rate of decay of the turbulent pressure producing structures was more rapid in the adverse case, and slower in the favorable case, in comparison with the zero pressure gradient case. The rms levels were greater in the adverse case and lower in the favorable case, relative to the zero case. Schloemer also concluded that an outer variable scaling was more effective than a mixed inner and outer variable scaling for collapsing the autospectra with other investigations at zero pressure gradient. Here, we investigate the scaling of the autospectra and convection velocities measured by Schloemer and estimate the wave number frequency spectrum for each pressure gradient case by transforming Schloemer's cross-spectral measurements in the spatial domain. We also consider the fundamental problem of the estimation of wave number frequency spectra from data obtained with a limited number of unequally spaced sensors. The results obtained regarding this method are applicable to measurements of other turbulence quantities, in addition to wall pressure.

II. Analysis and Results

Before direct measurements with large arrays of equally spaced transducers, estimates of the wave number frequency spectrum were obtained from measurements of the cross spectrum made with a relatively small number of transducers with unequal spacing. For

Received 13 December 1999; revision received 24 March 2000; accepted for publication 27 March 2000.

*Mechanical Engineer, Submarine Sonar Department, Code 2141, 1176 Howell Street. Member AIAA.

†Mechanical Engineer, Submarine Sonar Department, Code 2141, 1176 Howell Street. Associate Fellow AIAA.

a particular frequency ω_o, the wave number frequency spectrum, $\Phi(k, \omega_o)$, is related to the cross spectrum, $G(\xi, \omega_o)$, by

$$\Phi(k, \omega_o) = \frac{1}{2\pi} \int_{-\infty}^{\infty} G(\xi, \omega_o) e^{-ik\xi} \, d\xi \tag{1}$$

The work of Corcos[13] established the similarity scaling of the cross spectrum of the wall pressure field as $\zeta = |\omega\xi / u_c|$, with ξ the streamwise spatial coordinate and u_c the convection velocity. For fixed frequency ω_o, Corcos's model may be written

$$G(\xi, \omega_o) = \Phi(\omega_o) e^{-(i + \alpha)\zeta} \tag{2}$$

where $\Phi(\omega_o)$ represents the autospectrum evaluated at ω_o, and α is a decay constant for the cross spectrum. We note that Eq. (2) does not explicitly involve any turbulent boundary layer parameters. The measurements of Farabee and Casarella[2] that related analyses showed that the similarity scaling was only valid over a limited frequency range and was inadequate at low frequencies. Corcos's model, Eq. (2), provided an analytical expression that was transformed by other investigators to obtain a closed form expression for the wave number frequency spectrum. Keith and Abraham[4] showed that the variation of the convection velocity u_c with spatial separation ξ must be taken into account when estimating the wave number frequency spectrum from cross-spectral measurements by transforming Corcos's model, Eq. (2). The similarity variable then becomes

$$\zeta = \omega_o \xi / u_c(\xi, \omega_o) \tag{3}$$

To estimate $\Phi(k, \omega_o)$ from Eqs. (1) through (3), the quantities $\Phi(\omega_o)$, $\alpha(\omega_o)$, and $u_c(\xi, \omega_o)$ must be established. We nondimensionalize variables following Farabee and Casarella[2] and Keith et al.,[3] with the boundary thickness δ as the outer length scale, and δ / U_o as the outer time scale. The length scale δ is exact, as opposed to the displacement thickness δ^* or momentum thickness θ, which constitute integral length scales. We justify the use of outer variables based on the chosen (low) frequency ω_o, as discussed by Farabee and Casarella,[2] and also in view of Schloemer's conclusions. Defining $\chi = \xi / \delta$, $\psi = u_c(\chi, \omega_o) / U_o$, $\Omega_o = \omega_o \delta / U_o$, and $\kappa = k\delta$, the similarity scaling becomes $\zeta = |\Omega_o \chi / \psi|$. Equation (2) is then expressed as

$$\tilde{G}(\chi, \Omega_o) = \tilde{\Phi}(\Omega_o) e^{-(i + \tilde{\alpha})\zeta} \tag{4}$$

and Eq. (1) as

$$\tilde{\Phi}(\kappa, \Omega_o) = \frac{1}{2\pi} \int_{-\infty}^{\infty} \tilde{G}(\chi, \Omega_o) e^{-i\kappa\chi} \, d\chi \tag{5}$$

Under the incorrect assumption that u_c does not depend explicitly upon χ, Eq. (5) may be evaluated in closed form to obtain an estimate for $\tilde{\Phi}(\kappa, \Omega_o)$. This estimate was shown by Keith and Abraham[4] to inaccurately yield a symmetric convective ridge centered around the convective wave number, and high levels at low wave numbers. Many investigators have used this type of estimate for problems of flow induced noise and vibration. The errors resulting in these analyses are a direct result of the assumption of constant convection velocity with spatial separation when transforming the cross spectra. Although this type of estimate has been commonly referred to as the Corcos model, it should be noted that Corcos[13] did not transform his model of the cross spectra into the wave number domain and has not published a model for the wave number frequency spectra. When the dependence of convection velocity upon spatial separation is correctly taken into account, no closed-form solution for Eq. (5) is known to exist. Attempts to obtain a closed-form solution using the symbolic manipulation program Macsyma were unsuccessful. We therefore evaluate the transform numerically, using the MATLAB® fast Fourier transform algorithm, and also with a conventional Simpson integration scheme for comparison. The exponential decay of the integrand causes it to approach zero for large absolute values of χ.

Values for $\tilde{G}$ were obtained from Schloemer[12] for zero, and mild favorable and adverse pressure gradient cases. To account for the dependence of $\tilde{\alpha}$ on χ, Schloemer's measurements for u_c / U_o, which he presented as a function of ξ / δ^*, were used. It was observed that

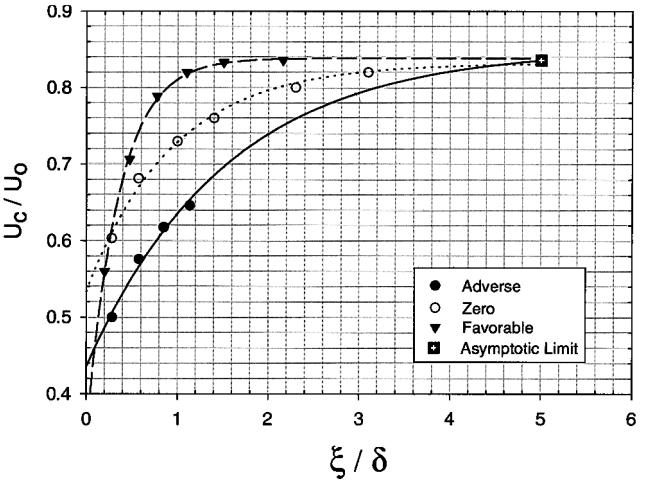

Fig. 1 Convection velocity vs longitudinal separation scaled with the boundary-layer thickness.

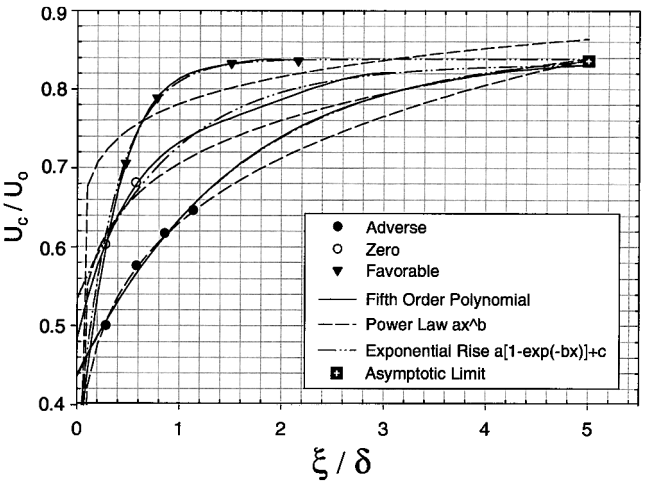

Fig. 2 Convection velocity vs longitudinal separation, showing different forms of curve fits.

scaling u_c / U_o with δ rather than δ^* resulted in a more clearly defined trend with varying pressure gradients, as presented in Fig. 1. This result supports the conclusions of Farabee and Casarella[2] that δ is, in general, a more accurate outer length scale than δ^* or θ. Here, the symbols represent values that were obtained directly from Schloemer[12] and rescaled, except for the data point at $\xi / \delta = 5.0$, which represents the value at which all three cases converge asymptotically. This point is denoted with a distinct symbol. The lines are curve fits through the data.

We note that the zero pressure gradient results for convection velocity agree well with subsequent investigations, as shown by Keith and Abraham.[4] Because of the extremely limited number of data points presented by Schloemer, however, several different forms of the curve fit were investigated. Figure 2 compares power law, fifth-order polynomial, and exponential fits for u_c / U_o with the original data for the zero pressure gradient case. Note that the polynomial and exponential curve fits are nearly coincident, whereas the power law has a slightly more gradual slope. The power law form was investigated based on the successful results of Keith and Abraham.[4] However, altering the form of the expression for the convection velocity had very little effect on the resulting wave number frequency spectrum, $\tilde{\Phi}(\kappa, \Omega_o)$, as evidenced in Fig. 3. The convective ridge is asymmetric, and its amplitude and convective wave number value are identical for the three cases shown. Also, for wave number values above the convective ridge, the results are reasonable and do not vary significantly with the form of the curve fit used in the calculation. Conversely, the dropouts observed for wave number values

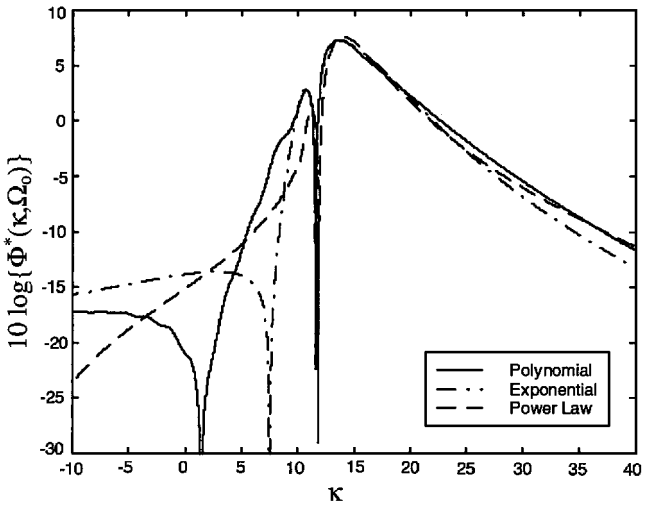

Fig. 3 Wave number frequency spectra for three curve fits for convection velocity: zero pressure gradient case only.

below the convective ridge are physically unrealistic and occur despite the form of the convection velocity curve. Subsequent attempts at removing these dropouts by further modifications to the transform function were unsuccessful. This failure is most likely due to the fact that the convection velocity data given by Schloemer is broadband rather than narrowband. Thus, these data represent an average due to contributions from the entire frequency range, rather than from the discrete frequency Ω_o.

The dominant trend in the convection velocity data is an increase in u_c as ξ increases and ω decreases. This trend is due to the spatial decay rates of the pressure producing turbulent structures, which are directly proportional to the distance of the structures from the wall. Larger structures at locations farther from the wall convect faster and are coherent over larger distances than those near the wall, as discussed by Keith and Abraham.[4] The speed at which these pressure producing turbulent structures convect is approximately equal to the mean velocity at the location of the structure in the turbulent boundary layer. In view of these results, a consistent trend is expected between the mean velocity data and convection velocity data for various pressure gradient cases. The velocity profile data of Schloemer[12] displays a distinct trend of steeper profiles with increasingly favorable pressure gradient. This trend is apparent in the convection velocity data of Fig. 1. This result reflects the use of δ as a more effective outer length scale. The discrete data points in Fig. 1 support these conclusions themselves, regardless of the curve fits used. It is readily apparent that the inner length scale ν/u_τ will not result in trends that are physically meaningful for the pressure gradient cases.

From Eqs. (4) and (5) it is apparent that the autospectral levels of $\tilde{\Phi}(\Omega_o)$ are required for the respective cases here. We extend the work of Schloemer,[12] seeking a collapse of the autospectra for the three cases using δ as an outer length scale. We note a reasonable collapse of the data for the three cases over the approximate frequency range $8 < \omega_o\delta/U_o < 18$, as shown in Fig. 4. At lower frequencies, an increase in spectral levels is apparent as the pressure gradient changes from favorable to adverse, consistent with Schloemer's conclusions. Clearly, a parameter involving the pressure gradient must be introduced to obtain a collapse in this low frequency region. Keith et al.[3] showed that, for higher frequency ranges where the effects of the finite sensor size are significant, conclusions as to the effectiveness of particular scalings for collapsing uncorrected data cannot be made. Schloemer applied the approximate correction method proposed by Corcos[13] to his autospectra. These results are shown in Fig. 5, where the outer variable scaling of Fig. 4 is again used. In Fig. 4, the lowest spectral levels are for the favorable case, which corresponds to the highest value of d/δ (Table 1), where d is the sensor diameter. However, the zero and adverse cases, which have approximately equal values of d/δ, do not collapse well. For the corrected results of Fig. 5, the adverse and favorable cases collapse at high frequencies,

Table 1 Boundary-layer parameters for favorable, zero, and adverse cases

Parameter	Favorable	Zero	Adverse
R_θ	1470	5800	9180
δ, mm	10.31	26.67	25.55
δ^*, mm	0.668	3.90	5.26
θ, mm	0.488	2.90	3.33
τ_w, Pa	6.063	1.860	1.998
θ/τ_w, dp/dx	−0.216	0.000	2.070
$d^+ = du_\tau/\nu$	216	119	124
d/δ	0.148	0.057	0.060
$\tilde{\Phi}(\Omega_o)$	1.35×10^{-7}	2.19×10^{-7}	3.24×10^{-7}

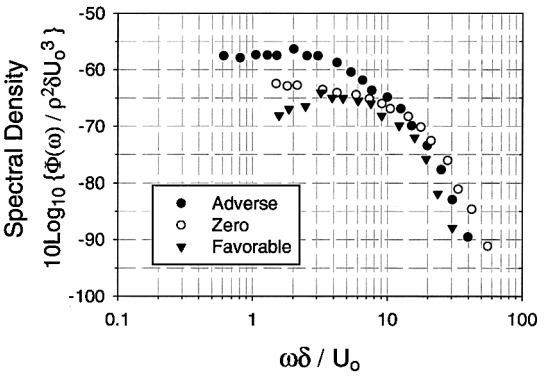

Fig. 4 Autospectral density scaled with outer variables.

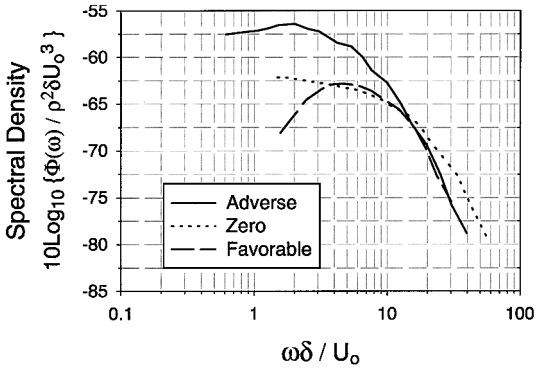

Fig. 5 Autospectral density, corrected for transducer size, scaled with outer variables.

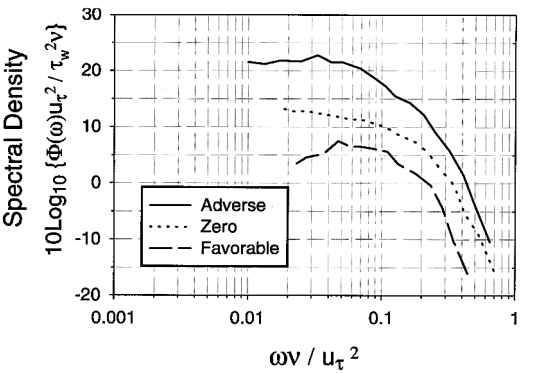

Fig. 6 Autospectral density scaled with inner variables.

but the zero case has notably higher levels. We conclude from these results that the outer variable scaling is ineffective in collapsing the data at higher frequencies.

Farabee and Casarella[2] concluded that for $\omega\nu/u_\tau^2 > 0.3$, an inner variable scaling effectively collapsed the autospectra for equilibrium turbulent boundary layers. The uncorrected spectra scaled on inner variables are shown in Fig. 6. The favorable case has the largest value of d^+ and exhibits the lowest levels, as one would expect. A

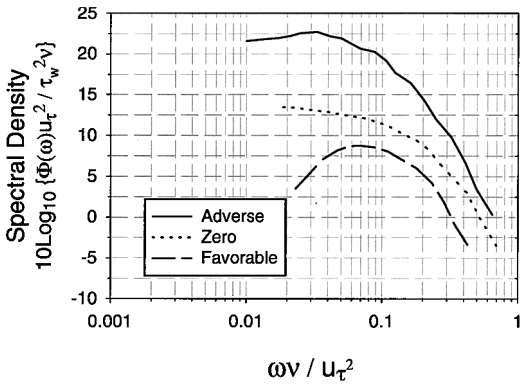

Fig. 7 Autospectral density, corrected for transducer size, scaled with inner variables.

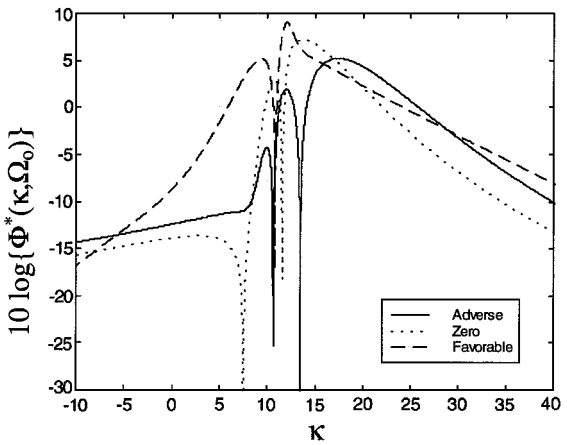

Fig. 8 Wave number frequency spectra for three pressure gradient cases.

near collapse of the zero and adverse cases is observed, where the values for d^+ are approximately the same. The corrected spectra scaled on inner variables are shown in Fig. 7. The same trends observed in Fig. 6 for the uncorrected case exist here. We conclude that a tight collapse of the data in the high frequency region requires a refinement in the correction for spatial averaging that accounts for pressure gradient effects on convection velocity. In addition, an explicit dependence on the pressure gradient parameter may be required.

In view of these results, we choose a value for $\omega_o \delta / U_o$ of 10, which lies within the frequency range where the autospectral data collapses with the outer variable scaling. The nondimensional spectral levels at this frequency are given in Table 1. Schloemer's cross-spectral measurements show that the similarity scaling proposed by Corcos collapses the streamwise cross-spectral data obtained at different speeds for the adverse case. The same holds for the favorable and zero cases. However, the different cases do not collapse with each other, as each has a unique exponential decay constant. The boundary layer parameters for the cases used here are summarized in Table 1.

To estimate $\tilde{\Phi}(\kappa, \Omega_o)$ from Eq. (5), the expressions resulting from the curve fits to the convection velocity data were used. The results for the three pressure gradient cases using the curve fits from Fig. 1 (exponential form) are shown in Fig. 8. Although the favorable and adverse cases had a larger number of convection velocity data points on which to base the curve fits, the severe dropouts observed in the resulting wave number frequency spectra for the zero case still exist. Again, while these features are physically unrealistic, their contribution to the overall energy levels are negligible. More important, a distinct trend is apparent: as the pressure gradient changes from favorable to adverse, the asymmetric convective ridge broadens, and its peak occurs at increasing values of wave number. The limited amount of data precludes conclusions regarding the low wave number region.

The results presented exhibit narrowband dropouts in the wave number region, thereby establishing the extreme sensitivity to the cross-spectral magnitude and phase data that are transformed in the spatial domain. Clearly, the curve fits used here lead to errors in the resulting wave number frequency spectra. The exponential decay constants for the magnitude of the cross spectra were taken directly from Schloemer's data. The use of a functional form other than exponential might lead to improvements in the wave number frequency spectra. However, this change would be an abandonment of the basic Corcos model, which Schloemer showed to be effective. Therefore, it is concluded that sufficiently accurate estimates in the subconvective and low wave number region were not obtained.

III. Conclusions

Estimations of the wave number frequency spectra are obtained for turbulent boundary layers with mild favorable and adverse pressure gradients from measurements of the fluctuating wall pressure field obtained by Schloemer.[12] The variation of convection velocity with spatial separation is taken into account for each case considered. A distinct trend in these spectra are displayed, with an asymmetric convective ridge that broadens as the pressure gradient changes from favorable to adverse. The boundary layer thickness δ is shown to be a more effective outer length scale than the momentum thickness δ^*, and its use leads to a clear trend in the convection velocity data. Furthermore, scaling the autospectra for the respective cases with outer variables causes a collapse of the data over a narrow frequency range. The effects of spatial averaging due to the finite transducer size are taken into account. An approximate collapse of the high frequency data is obtained for the adverse and zero pressure gradient cases with the inner variable scaling.

Formulating conclusions regarding the low wave number region of the spectra is difficult without more data at the outset. The limited number of spectral data leads to uncertainty in the calculations. A larger number of sensors would provide more cross-spectral data and enable refinement of the decay constant for each case. Contemporary technology using arrays with large numbers of sensors enables significantly more detailed measurements of the fluctuating wall pressure field, and its use would help clarify the results presented here. In view of this, Schloemer's experiment should be repeated with an array of sensors to fully ascertain the effects of pressure gradients on turbulent boundary layer wave number frequency spectra.

Acknowledgment

This research was supported by the In-House Laboratory Independent Research Program, Manager Richard Philips, Code 102, Naval Undersea Warfare Center, Division Newport, Project A622030.

References

[1] Willmarth, W. W., "Pressure Fluctuations Beneath Turbulent Boundary Layers," *Annual Review of Fluid Mechanics*, Vol. 7, 1975, pp. 13–38.

[2] Farabee, T. M., and Casarella, M. J., "Spectral Features of Wall Pressure Fluctuations Beneath Turbulent Boundary Layers," *Physics of Fluids A*, Vol. 3, No. 10, 1991, pp. 2410–2419.

[3] Keith, W. L., Hurdis, D. A., and Abraham, B. M., "A Comparison of Turbulent Boundary Layer Wall Pressure Spectra," *Journal of Fluids Engineering*, Vol. 114, No. 3, 1992, pp. 338–347.

[4] Keith, W. L., and Abraham, B. M., "Effects of Convection and Decay of Turbulence on the Wall Pressure Wavenumber-Frequency Spectrum," *Journal of Fluids Engineering*, Vol. 119, March 1997, pp. 50–55.

[5] Abraham, B. M., and Keith, W. L., "Direct Measurements of Turbulent Boundary Layer Wall Pressure Wavenumber-Frequency Spectra," *Journal of Fluids Engineering*, Vol. 120, March 1998, pp. 29–39.

[6] Bull, M. K., and Thomas, A. S. W., "High Frequency Wall Pressure Fluctuations in Turbulent Boundary Layers," *Physics of Fluids*, Vol. 19, No. 4, 1976, pp. 597–599.

[7] Schewe, G., "On the Structure and Resolution of Wall-Pressure Fluctuations Associated with Turbulent Boundary-Layer Flow," *Journal of Fluid Mechanics*, Vol. 134, 1983, pp. 311–328.

[8] Löfdahl, L., Kälvesten, E., and Stemme, G., "Small Silicon Pressure Transducers for Space–Time Correlation Measurements in a Flat Plate Boundary Layer," *Journal of Fluids Engineering*, Vol. 118, No. 3, 1996, pp. 457–463.

[9]Willmarth, W. W., and Yang, C. W., "Wall Pressure Fluctuations Beneath Turbulent Boundary Layers on a Flat Plate and a Cylinder," *Journal of Fluid Mechanics*, Vol. 41, 1970, pp. 47–80.

[10]Lueptow, R. M., "Turbulent Boundary Layer on a Cylinder in Axial Flow," Naval Underwater Systems Center Detachment, NUSC TR 8389, New London, CT, Sept. 1988.

[11]Snarski, S. R., and Lueptow, R. M., "Wall Pressure and Coherent Structures in a Turbulent Boundary Layer on a Cylinder in Axial Flow," *Journal of Fluid Mechanics*, Vol. 286, 1995, pp. 137–171.

[12]Schloemer, H. H., "Effects of Pressure Gradients on Turbulent-Boundary-Layer Wall-Pressure Fluctuations," *Journal of the Acoustical Society of America*, Vol. 42, No. 1, 1967, pp. 93–113.

[13]Corcos, G. M., "Resolution of Pressure in Turbulence," *Journal of the Acoustical Society of America*, Vol. 35, No. 2, 1963, pp. 192–199.

R. M. C. So
Associate Editor